ISSN: 1392-6292/ eISSN: 1648-3510

VILNIUS TECH Vilnius Gediminas Technical University

MATHEMATICAL MODELLING and ANALYSIS

2026
Volume 31
Issue 3
Pages 499–520
https://doi.org/10.3846/mma.2026.24076

Mapped Legendre collocation methods for linear Volterra–Fredholm integral equations with delays on a semi-infinite interval

Sofiane Boutarcha[a], Azedine Rahmoune[b] ✉ and Ahmed Guechi[c]

[a] *Mathematical Analysis and Application Laboratory, Department of Mathematics, Faculty of Mathematics and Informatics, University Mohamed El Bachir El Ibrahimi of Bordj Bou Arreridj, 34030 El-Anasser, Algeria*

[b] *Institute of Optics and Precision Mechanics, Setif 1 University-Ferhat Abbas, 19000 Setif, Algeria*

[c] *Department of Mathematics, University Center of Barika, Amdoukal Road, 05001 Barika, Algeria*

Article History:

- received June 5, 2025
- revised March 9, 2026
- accepted March 29, 2026

Abstract. In this paper, we present a collocation method for linear Volterra–Fredholm integral equations with delay on a semi-infinite interval. The method employs orthogonal mapped Legendre basis functions together with a mapped Gauss quadrature rule adapted to the Volterra operator, leading to a stable and well-conditioned linear system. The convergence properties of both the collocation and iterated collocation solutions are investigated in the L^2- and L^∞-norms, and algebraic convergence rates are derived under mild regularity assumptions. Several numerical examples are presented and discussed to show the accuracy and efficiency of the methods.

Keywords: Volterra–Fredholm integral equations; delay term, mapped Legendre functions; semi-infinite interval; spectral collocation; convergence analysis.

AMS Subject Classification: 45A05; 65R20; 41A10; 65L60.

✉ Corresponding author. E-mail: azedine.rahmoune@univ-setif.dz

1 Introduction

Volterra–Fredholm integral equations (VFIEs) constitute a fundamental class of operator equations arising in applied sciences, including population dynamics [12, 15, 16, 17, 19], epidemiology [9, 10], engineering [13, 20], physics [1, 6, 8, 11], and economics [27]. In many such models, the system response depends not only on its present state but also on its history, leading to the appearance of delay terms in the unknown function. These delays substantially modify the analytical structure of the equation and impose additional challenges for its numerical treatment, especially when the problem is posed on an unbounded domain. Consequently, developing accurate and efficient numerical methods capable of simultaneously handling delay effects and unbounded domains, to our knowledge, remains largely unexplored. In this work, we consider the form of a linear VFIE with delay posed on the semi-infinite interval $\mathbb{R}_+$

$$u(x) = f(x) + \int_0^x g(x,t)u(t-\tau_1)\,dt + \int_0^\infty k(x,t)u(t-\tau_2)\,dt, \quad x \in \mathbb{R}_+, \tag{1.1}$$

subject to the initial history condition

$$u(x) = u_0(x), \quad x \in [-\tau_*, 0], \quad \tau_* := \max(\tau_1, \tau_2), \tag{1.2}$$

where $\tau_1, \tau_2 \geq 0$ are given delay parameters and $u_0 \in C([-\tau_*, 0])$. Throughout the paper, we will specify appropriate regularity assumptions on f and the kernels g and k whenever needed for the theoretical analysis. The Volterra term encodes the causal dependence of the solution on its past values, while the Fredholm term captures nonlocal interactions distributed over the entire domain. Equation (1.1) can be rewritten in operator form as follows:

$$u - \mathcal{T}u = f, \tag{1.3}$$

where the linear operator $\mathcal{T} := \mathcal{G} + \mathcal{K}$ is defined, for $u \in L^2(\mathbb{R}_+)$, by

$$(\mathcal{G}u)(x) = \int_0^x g(x,t)\,u(t-\tau_1)\,dt, \quad (\mathcal{K}u)(x) = \int_0^\infty k(x,t)\,u(t-\tau_2)\,dt.$$

It is well known that traditional discretization techniques, such as finite difference and finite element methods, often require domain truncation, which may compromise accuracy or stability. Spectral methods, however, have recently been extended to unbounded domains, where they achieve high-order accuracy with relatively few degrees of freedom [3, 5, 18, 24]. In particular, approaches based on mapped orthogonal polynomial systems have proven especially effective in handling unbounded domains without artificial truncation [14, 21, 22, 23, 26]. Nevertheless, variable integration limits in the Volterra term and shifts in the argument caused by the delay make direct application of standard spectral methods nontrivial.

In this article, we develop a collocation method for the numerical solution of Equation (1.1) with condition (1.2). The method employs orthogonal mapped Legendre functions (OMLFs) to construct a stable approximation basis on $\mathbb{R}_+$, combined with a mapped Legendre-Gauss quadrature rule tailored to the Volterra integral term. This yields a well-conditioned discrete system that accurately captures the effect of the delay. A rigorous convergence analysis is established for both the approximate and iterated solutions in the L^2- and L^∞-norms. For solutions in the weighted Sobolev-type space $\widetilde{B}^m(\mathbb{R}_+)$, the method achieves algebraic convergence. Numerical examples demonstrate its efficiency and confirm the theoretical rates.

The remainder of this article is organized as follows: Section 2 introduces the mapped Legendre basis and its approximation properties. Section 3 presents the collocation discretization and implementation. Section 4 provides the stability and convergence analysis. Section 5 reports numerical experiments. Finally, Section 6 draws the conclusion.

2 Orthogonal mapped Legendre functions (OMLFs)

In this section, we recall tools for approximation and interpolation based on OMLFs and present two fundamental lemmas, the first of which constitutes the theoretical cornerstone of our convergence analysis, while the second introduces a mapped quadrature specifically adapted to the Volterra operator.

2.1 Definition and some properties of OMLFs

The n-th degree Legendre polynomials, denoted by $P_n(y)$, can be defined by:

$$P_n(y) = \frac{1}{2^n n!}\frac{d^n}{dy^n}(y^2-1)^n, \quad n \geq 0, \quad y \in (-1,1).$$

They form an orthogonal set with respect to the $L^2(-1,1)$ inner product:

$$(P_n, P_m) = \int_{-1}^{1} P_n(y)P_m(y)dy = \frac{2}{2n+1}\delta_{nm}, \quad n,m \in \mathbb{N},$$

where δ_{nm} is the Kronecker delta symbol.

Let $L^2(\mathbb{R}_+)$ denotes the Hilbert space of all square integrable functions defined on $\mathbb{R}_+$, equipped with the following inner product and norm:

$$(u,v) = \int_0^\infty u(x)v(x)dx, \quad \|u\|_{L^2(\mathbb{R}_+)} = \sqrt{(u,u)}.$$

Consider the one-to-one transformation $x = \varphi_s(y) : (-1,1) \to \mathbb{R}_+$, explicitly invertible, namely,

$$y = \varphi_s^{-1}(x) = \phi_s(x), \quad x \in \mathbb{R}_+,$$

such that $\phi_s(0) = -1$, $\phi_s(\infty) = 1$ and satisfy

$$\frac{dx}{dy} = \varphi_s'(y) > 0, \quad y \in (-1,1),$$

where s is a positive scaling factor. The mapped Legendre functions can be defined as (see, e.g., [23]):

$$\mathcal{P}_n^s(x) = \mu_s(\phi_s(x))\, P_n(\phi_s(x)), \quad s > 0, \quad x \in \mathbb{R}_+, \tag{2.1}$$

where

$$\mu_s(y) = \frac{1}{\sqrt{\varphi_s'(y)}}.$$

They are orthogonal since we have

$$\int_0^\infty \mathcal{P}_n^s(x)\mathcal{P}_m^s(x)dx = \int_{-1}^{1} P_n(y)P_m(y)dy = \frac{2}{2n+1}\delta_{nm}, \quad n,m \in \mathbb{N},$$

and they form a complete $L^2(\mathbb{R}_+)$-orthogonal system.

2.2 Approximation by OMLFs

Given a positive integer N and let us denote by $\mathbb{V}_N^s$ the finite-dimensional approximation subspace of $L^2(\mathbb{R}_+)$ defined as follows:

$$\mathbb{V}_N^s := \{v \mid v(x) = \mu_s(\phi_s(x))\,\psi(\phi_s(x)), \quad \forall \psi \in \mathbb{P}_N\},$$

where $\mathbb{P}_N$ is the space of all polynomials of degree at most N, defined on the interval $(-1,1)$. From (2.1) we find that

$$\mathbb{V}_N^s := \operatorname{span}\{\mathcal{P}_n^s \,:\, n = 0,\ldots,N\}.$$

In order to derive the interpolation error for the OMLFs, we make use of the change of variables induced by the mapping $x = \varphi_s(y)$ with inverse $y = \phi_s(x)$. For a given function $u(x)$ defined on $\mathbb{R}_+$, we consider

$$U_s(y) := u(\varphi_s(y)), \quad y \in (-1,1),$$

and for convenience we introduce its normalized counterpart

$$\widehat{U}_s(y) := \frac{U_s(y)}{\mu_s(y)}, \quad \widehat{u}_s(x) := \widehat{U}_s(\phi_s(x)) = \frac{u(x)}{\mu_s(\phi_s(x))}, \tag{2.2}$$

so that the transformed differential operator can be defined as follows:

$$D_x u(x) := \theta_s(x)\,\frac{d}{dx}\widehat{u}_s(x), \quad \theta_s(x) := \frac{dx}{dy} = \frac{1}{\phi_s'(x)}.$$

By repeated application, we obtain

$$\begin{aligned} D_x^k u(x) &= \theta_s(x)\frac{d}{dx}\left(\theta_s(x)\frac{d}{dx}\left(\cdots\theta_s(x)\frac{d}{dx}\widehat{u}_s(x)\cdots\right)\right) \\ &= \partial_y^k \widehat{U}_s(y), \quad k = 0,1,\ldots. \end{aligned} \tag{2.3}$$

Now, we introduce the mapped Legendre-weighted Sobolev space

$$\widetilde{B}^m(\mathbb{R}_+) = \Big\{u \;:\; D_x^k u \in L^2_{w_s^k}(\mathbb{R}_+), \quad 0 \le k \le m\Big\},$$

equipped with the norm and semi-norm

$$\|u\|_{\widetilde{B}^m} = \left(\sum_{k=0}^{m} \|D_x^k u\|^2_{L^2_{w_s^k}(\mathbb{R}_+)}\right)^{1/2}, \quad |u|_{\widetilde{B}^m} = \|D_x^m u\|_{L^2_{w_s^m}(\mathbb{R}_+)},$$

where the anisotropic weight functions is given by

$$w_s^k(x) := \phi_s'(x)\,(1-\phi_s(x)^2)^k.$$

Additionally, if we denote by $\{\eta_i^s, \rho_i^s\}_{i=0}^N$, the set of mapped Legendre-Gauss quadrature nodes and weights, supported on the semi-infinite interval $\mathbb{R}_+$, then it is easy to verify that

$$\eta_i^s = \varphi_s(\sigma_i), \quad \rho_i^s = \omega_i \varphi_s'(\sigma_i), \quad i = 0,1,\ldots,N,$$

where $\{\sigma_i, \omega_i\}_{i=0}^{N}$ denote the set of standard Legendre-Gauss quadrature nodes and weights. Thus, the discrete inner product in $C_b(\mathbb{R}_+)$, the space of bounded continuous functions on $\mathbb{R}_+$, and its associated norm are defined by

$$(u, v)_N = \sum_{i=0}^{N} u(\eta_i^s)v(\eta_i^s)\rho_i^s, \quad \|u\|_N = \sqrt{(u, u)_N}. \tag{2.4}$$

The mapped Legendre-Gauss interpolation operator $I_N^s : C_b(\mathbb{R}_+) \to \mathbb{V}_N^s$, associated with $\{\eta_i^s\}$, is given by

$$I_N^s u(\eta_i^s) = u(\eta_i^s), \quad i = 0, 1, \ldots, N,$$

and for $u \in C_b(\mathbb{R}_+)$, we can write

$$I_N^s u(x) = \sum_{n=0}^{N} \tilde{u}_n^s \mathcal{P}_n^s(x),$$

such that

$$\tilde{u}_n^s = \frac{1}{\gamma_n} \sum_{i=0}^{N} u(\eta_i^s)\mathcal{P}_n^s(\eta_i^s)\rho_i^s.$$

We have the following lemma:

Lemma 1. *For any $u \in \widetilde{B}^m(\mathbb{R}_+)$ with $m \geq 0$, we have*

$$\|I_N^s u - u\|_{L^2(\mathbb{R}_+)} \leq cN^{-m}|u|_{\widetilde{B}^m}, \tag{2.5}$$

$$\|I_N^s u - u\|_{L^\infty(\mathbb{R}_+)} \leq cN^{-(m-\frac{3}{4})}|u|_{\widetilde{B}^m}, \tag{2.6}$$

where c is positive constant independent of N and u.

Proof. The proof of estimate (2.5) is derived in [23]. To derive estimate (2.6), we adopt the same strategy and employ the following pull-back identity

$$I_N^s u(x) = I_N^s u(\varphi_s(y)) = \mu_s(y)\, I_N\left\{\tfrac{U_s(y)}{\mu_s(y)}\right\} = \mu_s(y)\, I_N \widehat{U}_s(y), \tag{2.7}$$

where $y \in (-1, 1)$ and I_N is the standard degree-N Legendre interpolant (at Legendre-Gauss nodes). Hence for every $y \in (-1, 1)$, we have

$$\left|I_N^s u(\varphi_s(y)) - u(\varphi_s(y))\right| = \mu_s(y) \left|I_N \widehat{U}_s(y) - \widehat{U}_s(y)\right|.$$

Because $\mu_s(y)$ is continuous and strictly positive on $(-1, 1)$, it is in particular bounded above, let

$$c_1 = \sup_{y\in(-1,1)} \mu_s(y) < \infty.$$

Therefore, controlling the sup-norm of $I_N^s u - u$ on $\mathbb{R}_+$ is equivalent (up to constant factors) to controlling the sup-norm of $I_N \widehat{U}_s - \widehat{U}_s$ on $(-1, 1)$:

$$\|I_N^s u - u\|_{L^\infty(\mathbb{R}_+)} \leq c_1 \|I_N \widehat{U}_s - \widehat{U}_s\|_{L^\infty(-1,1)}. \tag{2.8}$$

According to the standard estimate for Legendre interpolation (see, e.g., [7]), there exists a constant $C > 0$ independent of N such that

$$\|I_N\widehat{U}_s - \widehat{U}_s\|_{L^\infty(-1,1)} \leq C\,N^{-(m-\frac{3}{4})}\|\partial_y^m\widehat{U}_s\|_{L^2_{(1-y^2)^m}(-1,1)}. \tag{2.9}$$

By definition of the mapped derivatives (2.3), we have

$$\partial_y^m\widehat{U}_s(y) = D_x^m u(x).$$

Hence,

$$\|\partial_y^m\widehat{U}_s\|^2_{L^2_{(1-y^2)^m}(-1,1)} = \int_{-1}^{1}|\partial_y^m\widehat{U}_s(y)|^2(1-y^2)^m dy = |u|^2_{\widetilde{B}^m}. \tag{2.10}$$

Then combining (2.9) and (2.10) gives

$$\|I_N\widehat{U}_s - \widehat{U}_s\|_{L^\infty(-1,1)} \leq C\,N^{-(m-\frac{3}{4})}|u|_{\widetilde{B}^m}.$$

Employing (2.8), we get

$$\|I_N^s u - u\|_{L^\infty(\mathbb{R}_+)} \leq c_1 C\,N^{-(m-\frac{3}{4})}|u|_{\widetilde{B}^m},$$

which is the claimed estimate, where $c = c_1C$.

In order to handle the variable upper limit of the Volterra operator within the Legendre-Gauss framework, we need to employ an affine function that linearly transforms the reference interval $(-1,1)$ into the interval $(-1,\phi_s(x))$ associated with the change of variables $t = \varphi_s(y)$. To this end, one can consider, the following mapping:

$$z(x,\theta) = \frac{\phi_s(x)+1}{2}\,\theta + \frac{\phi_s(x)-1}{2}, \quad \theta \in (-1,1).$$

Next, we have the following lemma: □

Lemma 2. *Let $\{\eta_i^s\}_{i=0}^N$ be the set of mapped Legendre-Gauss quadrature nodes on $\mathbb{R}_+$, which are the roots of $\mathcal{P}^s_{N+1}(x)$. Then, for every $u \in \mathbb{V}_N^s$ and $v \in \mathbb{V}^s_{N+1}$, the following quadrature identity holds:*

$$\int_0^{\eta_i^s} u(t)\,v(t)\,dt = \sum_{j=0}^{N} u\left(\tilde{\eta}_j^{s,i}\right)\,v\left(\tilde{\eta}_j^{s,i}\right)\,\tilde{\rho}_j^{s,i},$$

where the quadrature nodes and weights are given by

$$\tilde{\eta}_j^{s,i} = z(\eta_i^s,\sigma_j), \quad \tilde{\rho}_j^{s,i} = \frac{1+\sigma_j}{2}\,\varphi_s'(\tilde{\eta}_j^{s,i})\,\omega_j. \tag{2.11}$$

Proof. For every $(u,v) \in \mathbb{V}_N^s \times \mathbb{V}_{N+1}^s$ we can write

$$u(x) = \mu_s(\phi_s(x))\psi_N(\phi_s(x)), \quad v(x) = \mu_s(\phi_s(x))\psi_{N+1}(\phi_s(x)),$$

where $\psi_N \in \mathbb{P}_N$ and $\psi_{N+1} \in \mathbb{P}_{N+1}$. Now, by setting $t = \varphi_s(z(x,\theta))$, we get

$$\phi_s(t) = \phi_s(\varphi_s(z(x;\theta))) = z(x,\theta), \quad (x,\theta) \in \mathbb{R}_+ \times (-1,1),$$

so that

$$\begin{aligned}\int_0^{\eta_i^s} u(t)v(t)dt &= \int_0^{\eta_i^s} \psi_N(\phi_s(t))\psi_{N+1}(\phi_s(t))\mu_s^2(\phi_s(t))dt \\ &= \int_{-1}^{1} \psi_N(z(\eta_i^s,\theta))\psi_{N+1}(z(\eta_i^s,\theta))z'(\eta_i^s,\theta)d\theta.\end{aligned}$$

Hence, by applying the Legendre-Gauss quadrature formula, yields

$$\begin{aligned}\int_0^{\eta_i^s} u(t)v(t)dt &= \sum_{j=0}^{N} \psi_N(z(\eta_i^s,\sigma_j))\psi_{N+1}(z(\eta_i^s,\sigma_j))\frac{1+\sigma_j}{2}\,\varphi_s'(\tilde{\eta}_j^{s,i})\,\omega_j \\ &= \sum_{j=0}^{N} u(\tilde{\eta}_j^{s,i})v(\tilde{\eta}_j^{s,i})\tilde{\rho}_j^{s,i},\end{aligned}$$

where $\tilde{\eta}_j^{s,i}$ and $\tilde{\rho}_j^{s,i}$ are defined in (2.11). □

It is now possible to derive a numerical scheme corresponding to Equation (1.1) with condition (1.2). For that, the associated kernels $g(x,t)$, $k(x,t)$, and the source term $f(x)$ are assumed to be continuous and bounded, with $u \in C_b(\mathbb{R}_+)$.

3 Discretization of VFIEs with delays

The spectral-collocation method based on the OMLFs is usually implemented in the physical space by seeking approximate solution to the Equation (1.1) supplemented with condition (1.2), in the form

$$u_N^s(x) = \sum_{n=0}^{N} \tilde{u}_n^s \mathcal{P}_n^s(x), \quad x \in \mathbb{R}_+, \tag{3.1}$$

with $u_N^s(x) = u_0(x)$ when $x \le 0$. In practice, this amounts to finding $u_N^s(x) \in \mathbb{V}_N^s$ such that the residual function

$$r_N(x) = u_N^s(x) - (\mathcal{G}u_N^s)(x) - (\mathcal{K}u_N^s)(x) - f(x)$$

is forced to vanish at the $(N+1)$ mapped Legendre-Gauss nodes. That is,

$$u_N^s(\eta_i^s) - (\mathcal{G}u_N^s)(\eta_i^s) - (\mathcal{K}u_N^s)(\eta_i^s) - f(\eta_i^s) = 0, \quad i = 0,1,\ldots,N. \tag{3.2}$$

To accomplish this, we must accurately approximate integral terms appearing in (3.2). Thanks to Lemma 2, the Volterra integral term can be effectively approximated at the i^{th} Legendre-Gauss node η_i^s as follows:

$$\begin{aligned}(\mathcal{G}u_N^s)(\eta_i^s) &\approx \sum_{j=0}^{N} g(\eta_i^s,\tilde{\eta}_j^{s,i})u_N^s(\tilde{\eta}_j^{s,i}-\tau_1)\tilde{\rho}_j^{s,i}\\ &\approx \sum_{j=0}^{q_i-1} g(\eta_i^s,\tilde{\eta}_j^{s,i})u_0(\hat{\eta}_j^{s,i})\tilde{\rho}_j^{s,i} + \sum_{j=q_i}^{N} g(\eta_i^s,\tilde{\eta}_j^{s,i})u_N^s(\hat{\eta}_j^{s,i})\tilde{\rho}_j^{s,i}, \end{aligned} \tag{3.3}$$

where $\hat{\eta}_j^{s,i} := \tilde{\eta}_j^{s,i} - \tau_1 < 0$ for all $j = 0,\ldots,q_i-1$. Similarly, the Fredholm integral term can be approximated by using the mapped Legendre-Gauss quadrature rule as:

$$\begin{aligned}(\mathcal{K}u_N^s)(\eta_i^s) &\approx \sum_{j=0}^{N} k(\eta_i^s,\eta_j^s)u_N^s(\eta_j^s-\tau_2)\rho_j^s\\ &\approx \sum_{j=0}^{r-1} k(\eta_i^s,\eta_j^s)u_0(\hat{\eta}_j^s)\rho_j^s + \sum_{j=r}^{N} k(\eta_i^s,\eta_j^s)u_N^s(\hat{\eta}_j^s)\rho_j^s, \end{aligned} \tag{3.4}$$

where $\hat{\eta}_j^s := \eta_j^s - \tau_2 < 0$ for all $j = 0,\ldots,r-1$. Hence, inserting (3.1) and the above two Equations (3.3)–(3.4) into (3.2) leads to the linear system

$$\begin{aligned}\sum_{n=0}^{N} \tilde{u}_n^s\mathcal{P}_n^s(\eta_i^s) - \sum_{j=0}^{q_i-1} g(\eta_i^s,\tilde{\eta}_j^{s,i})u_0(\hat{\eta}_j^{s,i})\tilde{\rho}_j^{s,i} - \sum_{n=0}^{N}\tilde{u}_n^s\sum_{j=q_i}^{N} g(\eta_i^s,\tilde{\eta}_j^{s,i})\mathcal{P}_n^s(\hat{\eta}_j^{s,i})\tilde{\rho}_j^{s,i}\\ - \sum_{j=0}^{r-1} k(\eta_i^s,\eta_j^s)u_0(\hat{\eta}_j^s)\rho_j^s - \sum_{n=0}^{N}\tilde{u}_n^s\sum_{j=r}^{N} k(\eta_i^s,\eta_j^s)\mathcal{P}_n^s(\hat{\eta}_j^s)\rho_j^s = f(\eta_i^s). \end{aligned} \tag{3.5}$$

Let us denote

$$\begin{aligned} g_{ij} &= g(\eta_i^s,\tilde{\eta}_j^{s,i}), \quad k_{ij} = k(\eta_i^s,\eta_j^s),\\ f_i &= f(\eta_i^s) + \sum_{j=0}^{q_i-1} g_{ij}u_0(\hat{\eta}_j^{s,i})\tilde{\rho}_j^{s,i} + \sum_{j=0}^{r-1} k_{ij}u_0(\hat{\eta}_j^s)\rho_j^s. \end{aligned}$$

Then (3.5) can be written as

$$\sum_{n=0}^{N}\tilde{u}_n^s\left[\mathcal{P}_n^s(\eta_i^s) - \sum_{j=q_i}^{N} g_{ij}\mathcal{P}_n^s(\hat{\eta}_j^{s,i})\tilde{\rho}_j^{s,i} - \sum_{j=r}^{N} k_{ij}\mathcal{P}_n^s(\hat{\eta}_j^s)\rho_j^s\right] = f_i,\ i = 0,\ldots,N,$$

which is an $(N+1)\times(N+1)$ matrix equations of the form

$$\left(\mathbf{P} - \sum_{i=0}^{N}\mathbf{G}_i\mathbf{W}_i\tilde{\mathbf{P}}_i - \mathbf{K}\mathbf{W}\hat{\mathbf{P}}\right)\mathbf{U} = \mathbf{F},$$

where

$$\mathbf{U} = (\tilde{u}_0^s,\ldots,\tilde{u}_N^s)^{\mathrm{T}}, \quad \mathbf{F} = (f_0,\ldots,f_N)^{\mathrm{T}}, \quad \mathbf{P} = \left[\mathcal{P}_n^s(\eta_i^s)\right]_{0\le i,n\le N},$$

$$\mathbf{G}_i = \begin{pmatrix} 0 & \cdots & 0 & 0 & \cdots & 0 \\ \vdots & & \vdots & \vdots & & \vdots \\ 0 & \cdots & 0 & 0 & \cdots & 0 \\ 0 & \cdots & 0 & g_{i,q_i} & \cdots & g_{i,N} \\ 0 & \cdots & 0 & 0 & \cdots & 0 \\ \vdots & & \vdots & \vdots & & \vdots \\ 0 & \cdots & 0 & 0 & \cdots & 0 \end{pmatrix}, \quad \tilde{\mathbf{P}}_i = \begin{pmatrix} 0 & 0 & \cdots & 0 \\ \vdots & \vdots & & \vdots \\ 0 & 0 & \cdots & 0 \\ \mathcal{P}_0^s(\hat{\eta}_{q_i}^{s,i}) & \mathcal{P}_1^s(\hat{\eta}_{q_i}^{s,i}) & \cdots & \mathcal{P}_N^s(\hat{\eta}_{q_i}^{s,i}) \\ \vdots & \vdots & & \vdots \\ \mathcal{P}_0^s(\hat{\eta}_N^{s,i}) & \mathcal{P}_1^s(\hat{\eta}_N^{s,i}) & \cdots & \mathcal{P}_N^s(\hat{\eta}_N^{s,i}) \end{pmatrix},$$

$$\mathbf{K} = \begin{pmatrix} 0 & \cdots & 0 & k_{0r} & \cdots & k_{0N} \\ 0 & \cdots & 0 & k_{1r} & \cdots & k_{1N} \\ \vdots & & \vdots & \vdots & & \vdots \\ 0 & \cdots & 0 & k_{Nr} & \cdots & k_{NN} \end{pmatrix}, \quad \hat{\mathbf{P}} = \begin{pmatrix} 0 & 0 & \cdots & 0 \\ \vdots & \vdots & & \vdots \\ 0 & 0 & \cdots & 0 \\ \mathcal{P}_0^s(\hat{\eta}_r^s) & \mathcal{P}_1^s(\hat{\eta}_r^s) & \cdots & \mathcal{P}_N^s(\hat{\eta}_r^s) \\ \vdots & \vdots & & \vdots \\ \mathcal{P}_0^s(\hat{\eta}_N^s) & \mathcal{P}_1^s(\hat{\eta}_N^s) & \cdots & \mathcal{P}_N^s(\hat{\eta}_N^s) \end{pmatrix},$$

$$\mathbf{W}_i = \begin{pmatrix} 0 & & & & 0 \\ & \ddots & & & \\ & & 0 & & \\ & & & \tilde{\rho}_{q_i}^{s,i} & \\ & & & & \ddots & \\ 0 & & & & \tilde{\rho}_N^{s,i} \end{pmatrix} \quad \text{and} \quad \mathbf{W} = \begin{pmatrix} 0 & & & & 0 \\ & \ddots & & & \\ & & 0 & & \\ & & & \rho_r^s & \\ & & & & \ddots & \\ 0 & & & & \rho_N^s \end{pmatrix}.$$

4 Convergence analysis

In this section, we analyze the convergence of the numerical scheme introduced in the previous section. To this end, we consider the discrete problem:

$$u_N^s - I_N^s \mathcal{T} u_N^s = I_N^s f, \tag{4.1}$$

where $I_N^s : C_b(\mathbb{R}_+) \to \mathbb{V}_N^s$ denotes the mapped Legendre interpolation operator described in subsection 2.2. For some integer $m \geq 1$, we make the following regularity assumptions:

(A1) The functions $x \mapsto g(x,t)$ and $x \mapsto k(x,t)$ belong to $\widetilde{B}^m(\mathbb{R}_+)$ in the x-variable and there exists a nonnegative function $M \in L^1(\mathbb{R}_+) \cap L^2(\mathbb{R}_+)$ such that

$$|g(\cdot,t)|_{\widetilde{B}^m} \leq M(t), \quad |k(\cdot,t)|_{\widetilde{B}^m} \leq M(t), \quad \text{for a.e. } t \geq 0.$$

(A2) The exact solution u and the right-hand side f belong to $\widetilde{B}^m(\mathbb{R}_+)$.

(A3) The mapping φ_s is a C^m-diffeomorphism on $(-1,1)$, and the derivatives $\varphi_s^{(j)}$ exist and are bounded on $(-1,1)$ for $1 \leq j \leq m$, so that the quadrature and interpolation constructions in Section 2 are valid.

These mild assumptions are satisfied for kernels that are sufficiently smooth in x, decay in t, and for regular mappings, such as the exponential, algebraic, and logarithmic mappings [3]. An essential step is to show the stability of the interpolation operator I_N^s.

Lemma 3. *For any $u \in \widetilde{B}^1(\mathbb{R}_+)$, we have*

$$\|I_N^s u\|_{L^2(\mathbb{R}_+)} \le C\,(\|u\|_{L^2(\mathbb{R}_+)} + N^{-1}\,|u|_{\widetilde{B}^1}) \le C\,(1+N^{-1})\|u\|_{\widetilde{B}^1}.$$

Proof. Although the result can be easily obtained as a consequence of the triangle inequality applied to u and $I_N^s u - u$, together with Lemma 1, we adopt here the pull-back approach (Subsec. 2.2), as it better highlights the role of the mapping and the structure of the underlying approximation space,

$$\widehat{U}_s(y) := U_s(y)/\mu_s(y) = U_s(y)\sqrt{\varphi_s'(y)}, \quad y \in (-1,1).$$

By the change of variables $x = \varphi_s(y)$ and $\mu_s^2(y) = 1/\varphi_s'(y)$, we get

$$\|\widehat{U}_s\|^2_{L^2(-1,1)} = \int_{-1}^{1} U_s(y)^2 \varphi_s'(y)\,dy = \int_0^\infty u(x)^2\,dx = \|u\|^2_{L^2(\mathbb{R}_+)}. \tag{4.2}$$

Due to (2.7), and using again the change of variables, we find that

$$\|I_N^s u\|^2_{L^2(\mathbb{R}_+)} = \int_{-1}^{1} \big(\mu_s(y) I_N \widehat{U}_s(y)\big)^2 \varphi_s'(y)\,dy = \|I_N \widehat{U}_s\|^2_{L^2(-1,1)}.$$

From (2.10), one has

$$\|\partial_y \widehat{U}_s\|^2_{L^2_{1-y^2}(-1,1)} = |u|^2_{\widetilde{B}^1}. \tag{4.3}$$

In addition, the Lemma 3.8 of [25, p. 131] (see also [4, Chap. 3]), states that

$$\|I_N \widehat{U}_s\|_{L^2(-1,1)} \le C\,(\|\widehat{U}_s\|_{L^2(-1,1)} + N^{-1}\,\|\partial_y \widehat{U}_s\|_{L^2_{1-y^2}(-1,1)}).$$

Hence, employing (4.2)–(4.3) in the above estimate yields

$$\|I_N^s u\|_{L^2(\mathbb{R}_+)} \le C\,(\|u\|_{L^2(\mathbb{R}_+)} + N^{-1}|u|_{\widetilde{B}^1}).$$

□

We now recall the following theorem on projection methods from [2, p. 55].

Theorem 1. *Let $\{X_N\}_{N\ge 0}$ be a sequence of finite dimensional subspaces of a Banach space X, and let $\mathcal{T} : X \to X$ be bounded. Further assume $I - \mathcal{T} : X \to X$ is bijective, and let $P_N : X \to X_N$ be a bounded projection operator satisfying*

$$\|\mathcal{T} - P_N \mathcal{T}\| \to 0 \quad \textit{as } N \to \infty.$$

Then, for all sufficiently large N, the operator $(I - P_N\mathcal{T})$ is invertible and

$$\sup_{N\ge N_0} \|(I - P_N\mathcal{T})^{-1}\| < \infty.$$

Moreover, if u solves $(I-\mathcal{T})u = f$ and u_N solves $(I-P_N\mathcal{T})u_N = P_N f$, then,

$$\|u-u_N\| \le C\,\|u-P_N u\|,$$

with C independent of N.

In order to apply the aforementioned theorem to our context, it is necessary to determine whether $\|\mathcal{T}-I_N^s\mathcal{T}\| \to 0$ as $N\to\infty$. The subsequent two lemmas provide results that address this issue.

Lemma 4. *Assume the regularity assumptions* (A1)–(A3) *are satisfied for the problem* (1.1)–(1.2)*. Then, for all $N\ge 1$, we have*

$$\|(\mathcal{T}-I_N^s\mathcal{T})u\|_{L^2(\mathbb{R}_+)} \le C\,N^{-m}\left(\|u\|_{L^2(\mathbb{R}_+)} + \|u_0\|_{L^2([-\tau_*,0])}\right),$$

where C is a positive constant independent of N, u and u_0. Therefore,

$$\|\mathcal{T}-I_N^s\mathcal{T}\|_{L^2\to L^2} \to 0 \quad \text{as } N\to\infty.$$

Proof. Let $u\in L^2(\mathbb{R}_+)$ be arbitrary with history $u_0\in C([-\tau_*,0])$. Decompose

$$\mathcal{T}-I_N^s\mathcal{T} = (\mathcal{G}-I_N^s\mathcal{G}) + (\mathcal{K}-I_N^s\mathcal{K}), \tag{4.4}$$

where $\mathcal{G}$ and $\mathcal{K}$ are the Volterra and Fredholm operators, respectively. Bound each separately; focus on $\mathcal{G}$ (similar for $\mathcal{K}$). The error is

$$(\mathcal{G}-I_N^s\mathcal{G})u(x) = \int_0^x e_g(x,t)\,u(t-\tau_1)\,dt,$$

with $e_g(x,t) := g(x,t)-(I_N^s g(\cdot,t))(x)$. By Cauchy–Schwarz inequality, we have

$$\left|(\mathcal{G}-I_N^s\mathcal{G})u(x)\right| \le \Big(\int_0^\infty |e_g(x,t)|^2 dt\Big)^{1/2}\Big(\int_0^\infty |u(t-\tau_1)|^2 dt\Big)^{1/2}. \tag{4.5}$$

A change of variable gives

$$\int_0^\infty |u(t-\tau_1)|^2 dt = \int_{-\tau_1}^\infty |u(s)|^2 ds$$
$$= \int_0^\infty |u(s)|^2 ds + \int_{-\tau_1}^0 |u_0(s)|^2 ds \le \|u\|^2_{L^2(\mathbb{R}_+)} + \|u_0\|^2_{L^2([-\tau_*,0])}. \tag{4.6}$$

Thus, using the estimate (4.6), squaring inequality (4.5) and integrating over x, then applying Fubini's theorem, we obtain

$$\|(\mathcal{G}-I_N^s\mathcal{G})u\|^2_{L^2(\mathbb{R}_+)} \le \left(\|u\|^2_{L^2(\mathbb{R}_+)} + \|u_0\|^2_{L^2([-\tau_*,0])}\right)\int_0^\infty \|e_g(\cdot,t)\|^2_{L^2_x(\mathbb{R}_+)} dt,$$

so that the problem is reduced to estimating $\|e_g(\cdot,t)\|_{L^2_x(\mathbb{R}_+)}$. Thanks to (A1) and the interpolation estimate of Lemma 1 applied to x-variable, we have for every $t\ge 0$:

$$\|e_g(\cdot,t)\|_{L^2_x(\mathbb{R}_+)} \le C_{\text{int}} N^{-m} |g(\cdot,t)|_{\widetilde{B}^m} \le C_{\text{int}} N^{-m} M(t),$$

where C_{int} is independent of N and g. Integrating in t, we get

$$\int_0^\infty \|e_g(\cdot,t)\|^2_{L^2_x(\mathbb{R}_+)} dt \le C^2_{\text{int}} N^{-2m} \|M\|^2_{L^2(\mathbb{R}_+)}.$$

Hence, according to (4.4), by collecting the bounds, we obtain

$$\|(\mathcal{T} - I^s_N\mathcal{T})u\|_{L^2(\mathbb{R}_+)} \le CN^{-m}\left(\|u\|_{L^2(\mathbb{R}_+)} + \|u_0\|_{L^2([-\tau_*,0])}\right),$$

with $C = \sqrt{2}C_{\text{int}}\|M\|_{L^2(\mathbb{R}_+)}$. To establish convergence in the operator norm, recall that $u_0 \in C([-\tau_*, 0])$, as specified in the introduction following equation (1.2). Since the interval $[-\tau_*, 0]$ is compact, u_0 is bounded, ensuring that $\|u_0\|_{L^2([-\tau_*,0])}$ is a finite constant independent of both N and u. Taking the supremum over all u with $\|u\|_{L^2(\mathbb{R}_+)} = 1$ thus yields the desired limit, namely,

$$\|\mathcal{T} - I^s_N\mathcal{T}\|_{L^2\to L^2} \to 0 \quad \text{as } N \to \infty.$$

□

Lemma 5. *Assume the regularity assumptions* (A1)–(A3) *are satisfied for the problem* (1.1)–(1.2). *Then, for all $N \ge 1$, we have*

$$\|(\mathcal{T} - I^s_N\mathcal{T})u\|_{L^\infty(\mathbb{R}_+)} \le C\,N^{-(m-\frac{3}{4})}\left(\|u\|_{L^\infty(\mathbb{R}_+)} + \|u_0\|_{L^\infty([-\tau_*,0])}\right), \tag{4.7}$$

where C is a positive constant independent of N, u, and u_0. Therefore,

$$\|\mathcal{T} - I^s_N\mathcal{T}\|_{C_b\to C_b} \to 0 \quad \text{as } N \to \infty.$$

Proof. Consider an arbitrary $u \in C_b(\mathbb{R}_+)$ with history $u_0 \in C([-\tau_*, 0])$. By using the decomposition (4.4) we can derive bounds for each component separately. For the Volterra part, the error at any $x \ge 0$,

$$(\mathcal{G} - I^s_N\mathcal{G})u(x) = \int_0^x e_g(x,t)\,u(t-\tau_1)\,dt,$$

where $e_g(x,t)$ is defined in the proof of Lemma 4. Define $\eta_x = \min(x, \tau_1)$, so $t - \tau_1 < 0$ on $[0, \eta_x]$ and $t - \tau_1 \ge 0$ on $[\eta_x, x]$. Then,

$$\left|(\mathcal{G} - I^s_N\mathcal{G})u(x)\right| \le \int_0^{\eta_x} \left|e_g(x,t)\right| |u_0(t-\tau_1)|\,dt + \int_{\eta_x}^x \left|e_g(x,t)\right| |u(t-\tau_1)|\,dt.$$

Taking the supremum over $x \ge 0$ and applying the bounds

$$\|u(\cdot - \tau_1)\|_{L^\infty(\mathbb{R}_+)} \le \|u\|_{L^\infty(\mathbb{R}_+)}, \quad \|u_0(\cdot - \tau_1)\|_{L^\infty(-\tau_1,0]} \le \|u_0\|_{L^\infty([-\tau_*,0])},$$

we obtain

$$\|(\mathcal{G} - I^s_N\mathcal{G})u\|_{L^\infty(\mathbb{R}_+)} \le \left(\|u\|_{L^\infty(\mathbb{R}_+)} + \|u_0\|_{L^\infty([-\tau_*,0])}\right)\int_0^\infty \sup_{x\ge 0}\left|e_g(x,t)\right| dt.$$

Under assumption (A1) and the uniform interpolation error estimate (2.6) from Lemma 1, we have

$$\sup_{x\geq 0}\left|e_g(x,t)\right| \leq C_{\text{int}}\, N^{-(m-\frac{3}{4})}\, |g(\cdot,t)|_{\widetilde{B}^m} \leq C_{\text{int}}\, N^{-(m-\frac{3}{4})}\, M(t),$$

yielding

$$\int_0^\infty \sup_{x\geq 0}\left|e_g(x,t)\right| dt \leq C_{\text{int}}\, N^{-(m-\frac{3}{4})}\, \|M\|_{L^1(\mathbb{R}_+)},$$

so that

$$\|(\mathcal{G}-I_N^s\mathcal{G})u\|_{L^\infty(\mathbb{R}_+)} \leq C_{\text{int}}\, N^{-(m-\frac{3}{4})}\, \|M\|_{L^1(\mathbb{R}_+)} \left(\|u\|_{L^\infty(\mathbb{R}_+)}+\|u_0\|_{L^\infty([-\tau_*,0])}\right).$$

For the Fredholm part, the error is

$$(\mathcal{K}-I_N^s\mathcal{K})u(x) = \int_0^\infty e_k(x,t)\, u(t-\tau_2)\, dt,$$

with $e_k(x,t) = k(x,t) - (I_N^s k(.,t))(x)$. Splitting the integral at $t = \tau_2$ and proceeding analogously yields

$$\|(\mathcal{K}-I_N^s\mathcal{K})u\|_{L^\infty(\mathbb{R}_+)} \leq C_{\text{int}}\, N^{-(m-\frac{3}{4})}\, \|M\|_{L^1(\mathbb{R}_+)} \left(\|u\|_{L^\infty(\mathbb{R}_+)}+\|u_0\|_{L^\infty([-\tau_*,0])}\right).$$

Summing the bounds for $\mathcal{G}$ and $\mathcal{K}$ gives (4.7), with C a possibly larger constant independent of N, u and u_0. For the operator norm convergence, recall that $u_0 \in C([-\tau_*,0])$ on a compact interval, implying $\|u_0\|_{L^\infty([-\tau_*,0])}$ is finite and independent of N and u. Taking the supremum over all $u \in C_b(\mathbb{R}_+)$ with $\|u\|_{L^\infty(\mathbb{R}_+)} = 1$ ensures the norm tends to zero as $N \to \infty$. □

Theorem 2. *Assume the regularity assumptions* (A1)–(A3) *are satisfied and that the problem* (1.1)–(1.2) *is uniquely solvable. Let* $u_N^s \in \mathbb{V}_N^s$ *be the discrete collocation solution determined by* (4.1)*, and* $\widetilde{u}_N^s$ *be the iterated collocation solution defined by*

$$\widetilde{u}_N^s := \mathcal{T}u_N^s + f.$$

Then, there exists $N_0 \geq 0$ *and a constant* $C > 0$*, independent of* N*, such that for all* $N \geq N_0$ *the operator* $(I - I_N^s\mathcal{T})$ *is invertible and the following estimates hold:*

$$\|u-u_N^s\|_{L^2(\mathbb{R}_+)} \leq C\, N^{-m}\, |u|_{\widetilde{B}^m},$$
$$\|u-\widetilde{u}_N^s\|_{L^2(\mathbb{R}_+)} \leq C\, \|\mathcal{T}\|\, N^{-m}\, |u|_{\widetilde{B}^m}.$$

Proof. From Equation (1.3), we have the following identity

$$I_N^s f = I_N^s((I-\mathcal{T})u) = I_N^s u - I_N^s\mathcal{T}u.$$

Then by using (4.1), we can write

$$\begin{aligned}(I-I_N^s\mathcal{T})(u-u_N^s) &= (I-I_N^s\mathcal{T})u - I_N^s f\\ &= u - I_N^s\mathcal{T}u - I_N^s f = u - I_N^s\mathcal{T}u - (I_N^s u - I_N^s\mathcal{T}u) = u - I_N^s u. \end{aligned} \tag{4.8}$$

The left-hand side of (4.8) involves the discrete operator $I - I_N^s \mathcal{T}$, while the right-hand side contains the pure interpolation error. Since $I - \mathcal{T}$ is bijective on $L^2(\mathbb{R}_+)$ and

$$\|\mathcal{T} - I_N^s \mathcal{T}\|_{L^2 \to L^2} \to 0 \quad \text{as } N \to \infty$$

by Lemma 4, Theorem 1 yields the existence of $N_0 \geq 0$ such that for all $N \geq N_0$ the operator $(I - I_N^s \mathcal{T})$ is invertible. Furthermore,

$$\|(I - I_N^s \mathcal{T})^{-1}\|_{L^2 \to L^2} \leq C, \tag{4.9}$$

for some constant $C > 0$, independent of N. This implies stability of the collocation system. Applying $(I - I_N^s \mathcal{T})^{-1}$ to (4.8) and using (4.9) yields

$$\|u - u_N^s\|_{L^2(\mathbb{R}_+)} \leq C\,\|u - I_N^s u\|_{L^2(\mathbb{R}_+)}. \tag{4.10}$$

Lemma 1 gives

$$\|u - I_N^s u\|_{L^2(\mathbb{R}_+)} \leq C\,N^{-m} |u|_{\widetilde{B}^m}, \tag{4.11}$$

where $|u|_{\widetilde{B}^m}$ denotes the highest-order weighted Sobolev seminorm associated with mapped derivatives. Combining (4.10) and (4.11) yields the asserted estimate for the collocation approximation:

$$\|u - u_N^s\|_{L^2(\mathbb{R}_+)} \leq C\,N^{-m}\,|u|_{\widetilde{B}^m}.$$

Finally, for the iterated approximation $\widetilde{u}_N^s = \mathcal{T} u_N^s + f$, we use the identity

$$u - \widetilde{u}_N^s = \mathcal{T}(u - u_N^s).$$

Since $\mathcal{T}$ is bounded in $L^2(\mathbb{R}_+)$, one obtains immediately

$$\|u - \widetilde{u}_N^s\|_{L^2(\mathbb{R}_+)} \leq \|\mathcal{T}\|_{L^2 \to L^2} \|u - u_N^s\|_{L^2(\mathbb{R}_+)} \leq C\|\mathcal{T}\| N^{-m} |u|_{\widetilde{B}^m}.$$

This completes the proof. □

Theorem 3. *Under the same assumptions as Theorem 2, the collocation and iterated collocation solutions satisfy the uniform-norm estimates:*

$$\|u - u_N^s\|_{L^\infty(\mathbb{R}_+)} = \mathcal{O}\big(N^{-(m-\frac{3}{4})}\big),$$
$$\|u - \widetilde{u}_N^s\|_{L^\infty(\mathbb{R}_+)} = \mathcal{O}\big(\|\mathcal{T}\| N^{-(m-\frac{3}{4})}\big).$$

The proof follows directly by the same arguments used in proving Theorem 2, with the L^2-based interpolation estimates replaced by the corresponding L^∞-bounds from Lemma 1 and Lemma 5, which together ensure the uniform invertibility of $I - I_N^s \mathcal{T}$ in $C_b(\mathbb{R}_+)$ and yield the stated convergence rates.

5 Illustrative examples

This section presents several numerical examples to confirm the theoretical results. All computations were carried out on an Intel(R) Core(TM) i5 processor running at 2.50 GHz with 4 GB of RAM, using a MATLAB R2009b program. The program is straightforward, requiring only the matrix operations detailed in Section 3. The implementation of our proposed approach is carried out by applying the following mappings between $x \in \mathbb{R}_+$ and $y \in (-1, 1)$ with $s > 0$:

i) Exponential mapping (EM):

$$\varphi_s(y) = -s\ln\frac{1-y}{2}, \quad \phi_s(x) = 1 - 2e^{-x/s}.$$

ii) Algebraic mapping (AM):

$$\varphi_s(y) = s\frac{1+y}{1-y}, \quad \phi_s(x) = \frac{x-s}{x+s}.$$

iii) Logarithmic mapping (LM):

$$\varphi_s(y) = \frac{s}{2}\ln\left(\frac{3+y}{1-y}\right), \quad \phi_s(x) = 2\tanh(x/s) - 1.$$

For notational convenience, we introduce

$$e_N^s := u - u_N^s \quad \text{and} \quad \tilde{e}_N^s := u - \widetilde{u}_N^s,$$

which denote the error functions of the approximate solution and the iterated solution, respectively, relative to the exact solution. Except Example 4, these errors are evaluated using the discrete L^2-norm, denoted by $\|.\|_{L^2}$, with respect to the mapped Legendre weight defined in (2.4), as well as the L^∞-norm, denoted by $\|.\|_\infty$, computed as the maximum absolute error (MAE) over a uniform grid of 1000 points on the interval $[0, 10]$. The columns labeled "*Ratio*" in following tables give the ratio of successive errors as:

$$Ratio \approx \frac{\log(\|e_N\|/\|e_{2N}\|)}{\log 2}.$$

Example 1. Consider the following delay problem:

$$\begin{cases} u(x) - 10\displaystyle\int_0^x te^{-t(x+1)}u(t-\tau)dt = f_\tau(x), & x \in \mathbb{R}_+, \quad \tau \geq 0, \\ u(x) = e^{-x}, \quad x \in [-\tau, 0], \end{cases}$$

where $f_\tau(x)$ is chosen so that the exact solution is $u(x) = e^{-x}$. Under the above mappings, the choice of the s-parameter is determined by the analyticity properties of the transformed function $\widehat{U}_s(y)$. Indeed, from (2.2), using the exponential mapping (EM), we find that

$$\widehat{U}_s(y) := \frac{u(\varphi_s(y))}{\mu_s(y)} = (\varphi_s'(y))^{-\frac{1}{2}}e^{-\varphi_s(y)} = 2^{-s}\sqrt{s}\,(1-y)^{s-\frac{1}{2}},$$

and when $s = r + \frac{1}{2}$, $r \in \mathbb{N}$, $\widehat{U}_s$ reduces to a polynomial of degree r. In this case, the interpolation operator is exact for $r \leq N$, yielding vanishing interpolation error (2.8). In particular, the selection ($s = \frac{3}{2}$) (corresponding to $r = 1$) ensures optimal theoretical accuracy for $N \geq 1$. It should be emphasized, however, that despite the polynomial character of the transformed solution for this choice, the associated kernel under the same mapping generally remains non-polynomial. Consequently, the full numerical scheme still involves non-polynomial contributions. Nevertheless, the mapped quadrature formula becomes increasingly effective as N increases, since higher-order interpolation enhances the resolution of the non-polynomial kernel and strengthens the overall convergence. Therefore, half-integer values of s, especially $s = \frac{3}{2}$, represent an optimal balance between theoretical exactness in the solution approximation and practical efficiency of the numerical method.

The results in Tables 1–2 and Figure 1 highlight the flexibility and robustness of the proposed method. While the first table show that EM achieves super-convergence when the scaling parameter s is optimally tuned, the second table and the figure reveal that with an arbitrary s the LM can outperform EM. This behavior demonstrates that the method is not rigidly dependent on a precise choice of s, but instead offers multiple effective mapping options, each capable of delivering high accuracy depending on the structure of the problem.

Table 1. MAEs and observed convergence rates for Example 1 with $\tau = 0.2$.

Appr.	EM		AM		LM	
N	$\lVert e_N^{\frac{3}{2}}\rVert_\infty$	*Ratio*	$\lVert e_N^{\frac{3}{2}}\rVert_\infty$	*Ratio*	$\lVert e_N^{\frac{3}{2}}\rVert_\infty$	*Ratio*
4	2.52×10^{-6}	–	8.68×10^{-3}	–	5.22×10^{-3}	–
8	4.94×10^{-13}	22.28	2.76×10^{-3}	1.65	2.19×10^{-3}	1.25
16	7.77×10^{-16}	9.31	1.29×10^{-4}	4.42	8.69×10^{-4}	1.33
Iter.	EM		AM		LM	
N	$\lVert \tilde{e}_N^{\frac{3}{2}}\rVert_\infty$	*Ratio*	$\lVert \tilde{e}_N^{\frac{3}{2}}\rVert_\infty$	*Ratio*	$\lVert \tilde{e}_N^{\frac{3}{2}}\rVert_\infty$	*Ratio*
4	1.64×10^{-7}	–	1.74×10^{-3}	–	3.75×10^{-4}	–
8	8.88×10^{-15}	24.14	3.10×10^{-4}	2.49	4.38×10^{-5}	3.10
16	1.89×10^{-15}	2.23	4.16×10^{-6}	6.22	6.25×10^{-6}	2.81

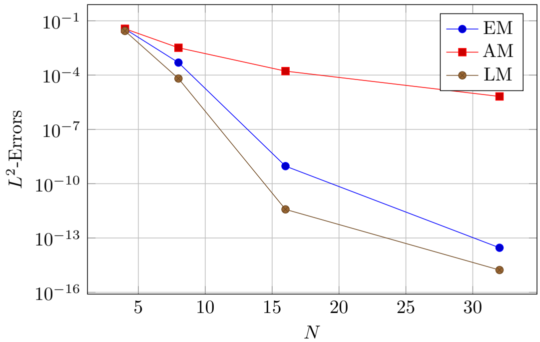

Figure 1. Convergence rates of EM, AM and LM methods obtained with $s = 3$ for Example 1 with $\tau = 1$.

Table 2. MAEs and observed convergence rates for Example 1 with $\tau = 2$.

Appr.	EM		AM		LM	
N	$\|e_N^3\|_\infty$	*Ratio*	$\|e_N^3\|_\infty$	*Ratio*	$\|e_N^3\|_\infty$	*Ratio*
8	3.75×10^{-3}	–	2.62×10^{-2}	–	5.82×10^{-4}	–
16	4.72×10^{-8}	16.21	2.01×10^{-3}	3.7	6.65×10^{-11}	23.06
32	8.71×10^{-10}	6.6	1.42×10^{-4}	3.83	8.55×10^{-15}	12.92
Iter.	EM		AM		LM	
N	$\|\tilde{e}_N^3\|_\infty$	*Ratio*	$\|\tilde{e}_N^3\|_\infty$	*Ratio*	$\|\tilde{e}_N^3\|_\infty$	*Ratio*
8	6.90×10^{-7}	–	1.27×10^{-5}	–	3.92×10^{-8}	–
16	1.38×10^{-11}	15.61	4.06×10^{-7}	4.96	7.99×10^{-15}	23.23
32	1.01×10^{-13}	7.09	2.76×10^{-8}	3.88	7.99×10^{-15}	0.00

Example 2. Consider the following delay problem:

$$u(x) - \int_0^x \frac{1}{(1+x)(1+t)} u(t-1)dt - \int_0^\infty \frac{xt}{((1+x^2)(1+t^2))^2} u(t-0.5)dt = f(x), \quad x \in \mathbb{R}_+,$$

with the initial condition

$$u(x) = \frac{1}{\sqrt{1+x^2}}, \quad x \in [-1, 0].$$

Here, $f(x)$ chosen so that the exact solution is $u(x) = \frac{1}{\sqrt{1+x^2}}$, which is smooth function and decays very slowly at infinity. Table 3 reports the L^2-errors and the maximum absolute errors versus N, obtained using algebraic mapping with different scaling parameters s. Clearly, as in Example 1, on can see that the iterative post-processing improve the obtained approximate solutions.

Example 3. Consider the linear Fredholm delay integral equation:

$$\begin{cases} u(x) - \displaystyle\int_0^\infty e^{-(x+t)} \cos(\omega t) u(t-1)dt = e^{-x}\left(1 - \frac{2e}{4+\omega^2}\right), & x \in \mathbb{R}_+, \\ u(x) = e^{-x}, \quad x \in [-1, 0], \end{cases}$$

where the exact solution is $u(x) = e^{-x}$ and the kernel $k(x,t)$ is smooth, highly oscillatory (controlled by $\omega > 0$), and exponentially decaying. Table 4 reports the maximum absolute errors for different fixed values of ω, obtained using the EM and LM methods. The results clearly demonstrate the superiority of EM over LM for semi-infinite, oscillatory Fredholm problems. Iterated solutions further improve accuracy, particularly for EM, confirming the effectiveness of the post-processing strategy. The exponential mapping achieves robust spectral convergence, even for high-frequency oscillations ($\omega = 10$), whereas LM requires significantly larger N to reach comparable accuracy.

Table 3. MAEs and L^2-errors with observed convergence rates for Example 2.

Appr.	AM					
N	$\Vert e_N^1\Vert_\infty$	*Ratio*	$\Vert e_N^1\Vert_{L^2}$	*Ratio*	$\Vert e_N^2\Vert_{L^2}$	*Ratio*
8	4.14×10^{-4}	–	1.61×10^{-5}	–	1.38×10^{-5}	–
16	3.79×10^{-7}	10.09	3.75×10^{-9}	12.1	2.26×10^{-8}	9.25
32	2.94×10^{-13}	20.3	3.53×10^{-15}	20.0	2.25×10^{-14}	19.94
Iter.	AM					
N	$\Vert \tilde{e}_N^1\Vert_\infty$	*Ratio*	$\Vert \tilde{e}_N^1\Vert_{L^2}$	*Ratio*	$\Vert \tilde{e}_N^2\Vert_{L^2}$	*Ratio*
8	3.85×10^{-6}	–	2.27×10^{-6}	–	4.12×10^{-6}	–
16	1.11×10^{-9}	11.76	5.27×10^{-10}	12.08	3.21×10^{-9}	10.32
32	6.11×10^{-16}	20.80	3.68×10^{-16}	20.02	8.11×10^{-15}	18.6

Table 4. MAEs using EM and LM methods for Example 3.

$\omega=2$	EM		LM	
N	$\Vert e_N^{5/2}\Vert_\infty$	$\Vert \tilde{e}_N^{5/2}\Vert_\infty$	$\Vert e_N^{5/2}\Vert_\infty$	$\Vert \tilde{e}_N^{5/2}\Vert_\infty$
8	1.57×10^{-5}	1.93×10^{-6}	1.39×10^{-4}	3.93×10^{-6}
16	4.14×10^{-8}	5.06×10^{-9}	3.02×10^{-5}	1.88×10^{-7}
32	2.40×10^{-11}	2.93×10^{-12}	4.04×10^{-6}	4.75×10^{-9}
64	5.37×10^{-14}	9.99×10^{-15}	7.57×10^{-7}	6.10×10^{-10}
$\omega=10$	EM		LM	
N	$\Vert e_N^{5/2}\Vert_\infty$	$\Vert \tilde{e}_N^{5/2}\Vert_\infty$	$\Vert e_N^{5/2}\Vert_\infty$	$\Vert \tilde{e}_N^{5/2}\Vert_\infty$
8	4.25×10^{-2}	5.41×10^{-4}	6.91×10^{-2}	8.31×10^{-4}
16	8.06×10^{-3}	1.02×10^{-4}	2.73×10^{-3}	3.29×10^{-5}
32	1.32×10^{-4}	1.68×10^{-6}	1.51×10^{-4}	1.99×10^{-6}
64	9.10×10^{-8}	1.71×10^{-9}	3.20×10^{-6}	1.47×10^{-7}

Example 4. [5] Finally, we consider the following problem without delay:

$$u(x)=\frac{|x-2|^{\frac{7}{2}}}{(x^2+2)^3}+\int_0^x \frac{e^{-\frac{t}{2}}\sin(\log(t^2+x+1))}{(x^2+t^2+2)^4}u(t)dt, \quad x\in\mathbb{R}_+,$$

whose exact solution is unknown. For the sake of comparison with the results in [5], obtained using the truncated Lagrange interpolation method combined with a truncated Gaussian quadrature formula, we compute the maximum absolute errors using the following weighted error measures

$$e_N = \max_{x\in[0,d]} \left|(u^s_{1024}(x) - u^s_N(x))w(x)\right|,$$
$$\tilde{e}_N = \max_{x\in[0,d]} \left|(\tilde{u}^s_{1024}(x) - \tilde{u}^s_N(x))w(x)\right|,$$

where $w(x) = x^\gamma(1+x)^\delta e^{-x/2}$. We take $d = 6$, $\gamma = 1/4$ and $\delta = 0$. Table 5 shows that the proposed method with $s = 5$ outperforms that of [5], achieving comparable accuracy at the approximate solution level (e_N) and significantly higher accuracy for iterated solutions, with gains of several orders of magnitude. It also converges faster and is more numerically efficient, especially when combined with the algebraic mapping (AM), which remains stable for large N (Table 6). Figure 2 confirms the convergence and stability of the method, ensuring the reliability of the numerical solutions.

The superior performance of AM arises from its alignment with the solution's algebraic decay. The kernel structure dominated by high-order algebraic denominators and the algebraically decaying nonhomogeneous term indicate that the exact solution decays algebraically rather than exponentially. Consequently, AM provides a natural asymptotic match on the semi-infinite domain, maintaining stable and high convergence rates as N increases.

Table 5. Comparison results for Example 4.

	[5]	EM	AM	LM
e_8	1.11×10^{-4}	1.52×10^{-2}	2.02×10^{-2}	1.16×10^{-2}
$\tilde{e}_8$	–	2.37×10^{-6}	3.59×10^{-6}	1.65×10^{-6}
e_{16}	3.79×10^{-5}	1.60×10^{-4}	3.17×10^{-4}	6.67×10^{-5}
$\tilde{e}_{16}$	–	1.19×10^{-8}	2.86×10^{-8}	3.82×10^{-9}
e_{32}	1.53×10^{-6}	1.38×10^{-6}	3.42×10^{-6}	5.18×10^{-7}
$\tilde{e}_{32}$	–	5.15×10^{-11}	1.38×10^{-10}	2.50×10^{-12}
e_{64}	7.91×10^{-8}	1.61×10^{-7}	2.80×10^{-7}	1.20×10^{-7}
$\tilde{e}_{64}$	–	3.43×10^{-13}	1.34×10^{-12}	2.09×10^{-12}
e_{128}	5.76×10^{-10}	1.04×10^{-8}	2.64×10^{-8}	3.16×10^{-8}
$\tilde{e}_{128}$	–	1.21×10^{-13}	3.90×10^{-14}	3.25×10^{-13}
e_{256}	4.14×10^{-11}	3.14×10^{-9}	2.78×10^{-9}	1.05×10^{-8}
$\tilde{e}_{256}$	–	1.43×10^{-14}	9.84×10^{-16}	5.34×10^{-14}
e_{512}	5.71×10^{-12}	1.05×10^{-9}	2.92×10^{-10}	3.21×10^{-9}
$\tilde{e}_{512}$	–	2.16×10^{-15}	7.07×10^{-17}	7.66×10^{-15}

Table 6. Convergence rates (*Ratio*) for EM, AM, and LM methods.

	EM		AM		LM	
N	Appr.	Iter.	Appr.	Iter.	Appr.	Iter.
$8 \to 16$	6.57	7.64	5.99	6.97	7.45	8.75
$16 \to 32$	6.86	7.85	6.53	7.69	7.01	10.58
$32 \to 64$	3.09	7.23	3.61	6.70	2.10	0.26
$64 \to 128$	3.97	1.53	3.42	5.12	1.93	2.68
$128 \to 256$	1.69	3.00	3.36	4.54	1.59	2.61
$256 \to 512$	1.68	2.32	1.81	1.20	1.71	2.80

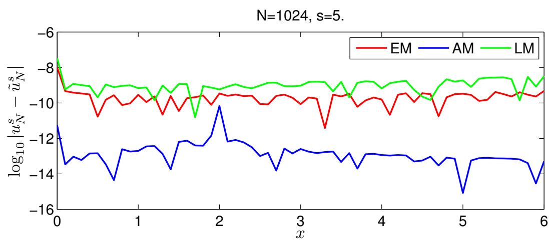

Figure 2. Additional numerical results for Example 4.

6 Conclusions

This work develops an efficient mapped Legendre collocation method for solving linear VFIEs with delays on the semi-infinite interval, an area where numerical challenges arise due to the presence of delay terms and the unbounded domain. By combining orthogonal mapped Legendre functions with a newly designed mapped Legendre-Gauss quadrature formula, the method achieves high accuracy while remaining computationally simple. A rigorous convergence analysis is provided, covering both the approximate and iterated solutions. The effectiveness and robustness of the approach are demonstrated through several representative examples, including cases with known and unknown exact solutions, showing clear advantages over existing numerical techniques. The paper therefore contributes a general, stable, and spectrally accurate framework for delayed integral equations on unbounded domains.

Acknowledgements

The authors express their gratitude to the anonymous reviewers for their careful reading of the manuscript and their many insightful comments and suggestions.

References

[1] R. Amin, K. Shah, M. Asif and I. Khan. Efficient numerical technique for solution of delay Volterra-Fredholm integral equations using Haar wavelet. *Heliyon*, **6**(10):e05108, 2020. https://doi.org/10.1016/j.heliyon.2020.e05108.

[2] K.E. Atkinson. *The Numerical Solution of Integral Equations of the Second Kind*, volume 4 of *Cambridge Monographs on Applied and Computational Mathematics*. Cambridge University Press, 1997. https://doi.org/10.1017/CBO9780511626340.

[3] S. Benyoussef and A. Rahmoune. Efficient spectral-collocation methods for a class of linear Fredholm integro-differential equations on the half-line. *J. Comput. Appl. Math.*, **377**:112894, 2020. https://doi.org/10.1016/j.cam.2020.112894.

[4] C. Bernardi and Y. Maday. Spectral methods. In *Techniques of Scientific Computing (Part 2)*, volume 5 of *Handbook of Numerical Analysis*, pp. 209–485. Elsevier, 1997. https://doi.org/10.1016/S1570-8659(97)80003-8.

[5] M.C. De Bonis, C. Laurita and V. Sagaria. A numerical method for linear Volterra integral equations on infinite intervals and its application to the resolution of metastatic tumor growth models. *Appl. Numer. Math.*, **172**:475–496, 2022. https://doi.org/10.1016/j.apnum.2021.10.015.

[6] B. Cahlon. On the numerical stability of Volterra integral equations with delay argument. *J. Comput. Appl. Math.*, **33**(1):97–104, 1990. https://doi.org/10.1016/0377-0427(90)90259-3.

[7] C. Canuto, M.Y. Hussaini, A. Quarteroni and T.A. Zang. *Spectral Methods: Fundamentals in Single Domains*. Scientific Computation. Springer, Berlin, Heidelberg, 2006. https://doi.org/10.1007/978-3-540-30726-6.

[8] J.M.F. Chamayou and M.E.A. El Tom. On the approximate solution of the delay integral equation of the statistical theory of radiation damage. *Comput. Phys. Commun.*, **9**(3):131–140, 1975. https://doi.org/10.1016/0010-4655(75)90102-2.

[9] K.L. Cooke. An epidemic equation with immigration. *Math. Biosci.*, **29**(1-2):135–158, 1976. https://doi.org/10.1016/0025-5564(76)90033-X.

[10] K.L. Cooke and J.L. Kaplan. A periodicity threshold theorem for epidemics and population growth. *Math. Biosci.*, **31**(1-2):87–104, 1976. https://doi.org/10.1016/0025-5564(76)90042-0.

[11] W.K. Ergen. Kinetics of the circulating-fuel nuclear reactor. *J. Appl. Phys.*, **25**(6):702–711, Jun 1954. https://doi.org/10.1063/1.1721720.

[12] W. Feller. On the integral equation of renewal theory. *Ann. Math. Statist.*, **12**(3):243–267, 1941. https://doi.org/10.1214/aoms/1177731708.

[13] E. Fridman. *Introduction to Time-Delay Systems: Analysis and Control*. Systems & Control: Foundations & Applications. Birkhäuser, Basel, Heidelberg, 2014. https://doi.org/10.1007/978-3-319-09393-2.

[14] A. Guechi and A. Rahmoune. Mapped Chebyshev spectral methods for solving second kind integral equations on the real line. *Aust. J. Math. Anal. Appl.*, **14**(2):12, 2017. Available from Internet: `https://ajmaa.org/searchroot/files/pdf/v14n2/v14i2p12.pdf`.

[15] J.M. Gushing. Volterra integrodifferential equations in population dynamics. In Mimmo Iannelli(Ed.), *Mathematics of biology*, C.I.M.E. Summer Schools, pp. 81–148. Springer, Berlin, Heidelberg, Sep 2011. https://doi.org/10.1007/978-3-642-11069-6_2.

[16] F.C. Hoppensteadt. *Mathematical Theories of Populations: Demographics, Genetics, and Epidemics*, volume 20 of *CBMS-NSF Regional Conference Series in Applied Mathematics*. Society for Industrial and Applied Mathematics, Philadelphia, 1975.

[17] M. Iannelli. *Mathematical Theory of Age-Structured Population Dynamics*. Applied Mathematics Monographs. Giardini editori e stampatori, Pisa, 1995.

[18] Ö.K. Kürkçü. An exclusive spectral computational approach based on quadratic orthoexponential polynomials for solving integro-differential equations with delays on the real line. *Appl. Numer. Math.*, **184**:1–17, 2023. https://doi.org/10.1016/j.apnum.2022.10.001.

[19] M. Mei, C.-K. Lin, C.-T. Lin and J.W.-H. So. Traveling wavefronts for time-delayed reaction–diffusion equation: (i) local nonlinearity. *J. Differ. Equ.*, **247**(2):495–510, 2009. https://doi.org/10.1016/j.jde.2008.12.026.

[20] S.I. Niculescu. *Delay Effects on Stability: A Robust Control Approach*, volume 269 of *Lecture Notes in Control and Information Sciences*. Springer-Verlag London, 2001. https://doi.org/10.1007/1-84628-553-4.

[21] A. Rahmoune. On the numerical solution of integral equations of the second kind over infinite intervals. *J. Appl. Math. Comput.*, **66**(1):129–148, 2021. https://doi.org/10.1007/s12190-020-01428-2.

[22] A. Rahmoune and A. Guechi. A rational spectral collocation method for solving Fredholm integral equations on the whole line. *Int. J. Comput. Sci. Math.*, **13**:32–41, 2021. https://doi.org/10.1504/IJCSM.2021.114184.

[23] W. Remili and A. Rahmoune. Modified Legendre rational and exponential collocation methods for solving nonlinear Hammerstein integral equations on the semi-infinite domain. *Int. J. Comput. Math.*, **99**(10):2018–2041, 2022. https://doi.org/10.1080/00207160.2022.2033236.

[24] W. Remili, A. Rahmoune and C. Li. Galerkin spectral method for linear second-kind Volterra integral equations with weakly singular kernels on large intervals. *Math. Methods Appl. Sci.*, **47**(4):2329–2344, 2022. https://doi.org/10.1002/mma.9750.

[25] J. Shen, T. Tang and L.-L. Wang. *Spectral Methods: Algorithms, Analysis and Applications*, volume 41 of *Springer Series in Computational Mathematics*. Springer, Berlin, Heidelberg, 2011. https://doi.org/10.1007/978-3-540-71041-7.

[26] T. Tang, L.-L. Wang, H. Yuan and T. Zhou. Rational spectral methods for PDEs involving fractional Laplacian in unbounded domains. *SIAM J. Sci. Comput.*, **42**(2):A585–A611, 2020. https://doi.org/10.1137/19M1244299.

[27] Y. Yatsenko. Volterra integral equations with unknown delay time. *Methods Appl. Anal.*, **2**(4):408–419, 1995. https://doi.org/10.4310/MAA.1995.v2.n4.a3.